

## Investigation of ZrO<sub>2</sub>-Y<sub>2</sub>O<sub>3</sub> Added Al Matrix Composites Produced by T/M Method

Serkan ÖZEL<sup>1\*</sup>, Tural HAMİDLİ<sup>1</sup>

<sup>1</sup>Bitlis Eren Üniversitesi, Mühendislik Mimarlık Fakültesi, Makine Müh. Böl., 13000, Bitlis  
(ORCID: [0000-0003-0700-1295](https://orcid.org/0000-0003-0700-1295)) (ORCID: [0000-0003-4200-0933](https://orcid.org/0000-0003-4200-0933))



**Keywords:** Powder Metallurgy, ZrO<sub>2</sub>-Y<sub>2</sub>O<sub>3</sub>, Al, Composite, Microstructure, Microhardness.

### Abstract

In this study, 5% by weight copper powder was added to the aluminum powder and this powder mixture was used as the matrix component. As a reinforcement element, 5%, 10%, and 15% ZrO<sub>2</sub>-Y<sub>2</sub>O<sub>3</sub> powder was mixed into the Al+ 5% Cu matrix component. The mixed powders were pressed unidirectional with 300MPa pressure to obtain powder metal samples. Pressed specimens were sintered at 500 °C. Optical microstructure and SEM images of sintered samples were taken. EDS, XRD, and microhardness analyzes were performed. According to the results obtained, the highest microhardness value was measured in the sample with 15% ZrO<sub>2</sub>-Y<sub>2</sub>O<sub>3</sub> powder sintered at 500 °C. In the XRD examination, it was determined that ZrO<sub>2</sub>, AlCu, Cu<sub>3</sub>Al, Al<sub>3</sub>Y and Al<sub>2</sub>O<sub>3</sub> compounds were also formed together with the Al main phase.

## 1. Introduction

Powder metallurgy is a technology that prepares high-performance materials by forming high metals, alloys, and composites with high yield and tensile strength, fine-grained, uniform structure, good thermal processing treatment, and isotropy [1]. With powder metallurgy technology, scrap losses can be reduced, material tolerances can be followed closely, complex-shaped products can be designed, and reproducibility can be allowed. [2]. Powder metallurgy includes processes such as mixing, pressing, and sintering of pre-alloyed or pre-mixed powders. In addition, it is a method that can be applied to many materials and is still under development [3].

The powder metallurgy method has many advantages over metal matrix composite methods. In this method, the matrix material (continuous phase) and reinforcement materials (discrete phases) are mixed and compressed under sufficient pressure and the green compact is formed. The green compacts are heated at a high temperature below the melting point of the matrix material for a sufficient time for diffusion bonding to occur. This process is also known as the sintering process. The powder

metallurgy process is most affected by the compaction pressure, holding temperature, and time parameters [4], [5], [6].

Many researchers have been working on aluminum matrix composites in recent years. These advanced composites are used in engineering applications, automotive, and aerospace industries. In addition to some reinforcements, intermetallics have also been found as reinforcement material for aluminum. Their coefficient of thermal expansion (CTE) is close to aluminum and less brittle than ceramic [7].

The packaging, automobile, defense, and aerospace industries highly demand Aluminum Matrix Composites (AMCs) or Aluminum-based Metal Matrix Composites (MMCs) due to their high strength, lightweight, and excellent tribological properties. These parameters play an important role in determining the properties of a powder metallurgy product. In addition, reinforcement materials are also effective in defining the properties of the composite material. The nature of the reinforcement materials and their bonding with the matrix material also affect the properties of composite materials. [4]. While aluminum matrix composite materials are produced by powder metallurgy, their strength can be

\*Corresponding author: [sozel@beu.edu.tr](mailto:sozel@beu.edu.tr)

Received: 31.08.2022, Accepted: 02.12.2022

increased with reinforcement particles such as SiC, Al<sub>2</sub>O<sub>3</sub>, ZrO<sub>2</sub>, MgO, B<sub>4</sub>C, TiB<sub>2</sub> [8]-[13].

Zirconium dioxide (ZrO<sub>2</sub>) can be widely used in high-tech engineering applications because it has remarkable properties such as the ability to work at high temperatures, resistance to corrosion and abrasion, high strength and fracture toughness, semiconductivity, thermal and diffusion barrier behavior, and biocompatibility [10]. Cubic zirconia (YSZ) stabilized with Ytria (Y<sub>2</sub>O<sub>3</sub>) is used in many fields such as aerospace, aviation, automobile, health, high-temperature turbine blades, and most importantly solid electrolyte [14]. YSZ has properties such as high melting point (~2700 °C), low thermal conductivity (~2.6W/m K), relatively low density (6.4 g cm<sup>-3</sup>), high hardness (14GPa), high resistance to atmospheric and high-temperature corrosion [15].

In this study, 5% by weight of copper powder was mixed with aluminum powder. As a reinforcement element, 5%, 10%, and 15% ZrO<sub>2</sub>-Y<sub>2</sub>O<sub>3</sub> powder was added to this matrix mixture powder. The effect of the reinforcement particle ratio on the samples after sintering at 500 °C was investigated.

## 2. Material and Method

In this study, Al powders were used as matrix material. The aluminium was used as a matrix with purity level were 99% manufactured by (Praxair Al-104, -90 µm/+45 particle size) and remaining are impurities. ZrO<sub>2</sub>-8% Y<sub>2</sub>O<sub>3</sub> (Ytria stabilized zirconia) powder was manufactured by Oerlikon Metco's (with 99.5% purity and -125 +11 µm particle size). 5% Cu powder (Alfa Aesar, -45 µm , 99%) was added to the Al powder. Prepared mixtures are shown in Table 1.

**Table 1.** Prepared powder mixes

Specimens	Matrix Powder (Al+5Cu)	Supplement powder (ZrO <sub>2</sub> -Y <sub>2</sub> O <sub>3</sub> )
1	%100	0
2	%95	%5
3	%90	%10
4	%85	%15

5%, 10%, and 15% ZrO<sub>2</sub>-Y<sub>2</sub>O<sub>3</sub> powders were added to the Al+5% Cu powder mixture as reinforcement material. For the homogeneous distribution of the powders, the mixing process was

carried out at a speed of 45 rpm in 45 minutes. Mixing of powders was carried out dry.

After mixing, each powder mixture was cold pressed unidirectionally at a pressure of 300 MPa with a size of 12 mm diameter. The sintering process was applied to the pressed samples in the Protherm brand furnace in the Advanced Research Laboratory of Bitlis Eren University (see Figure 1). Samples of each powder mixture were sintered at 500 °C for 60 minutes. The sintering temperature was chosen by examining the Al-Cu equilibrium diagram. The amount of Cu and temperature at which precipitation hardening can be achieved were selected.



**Figure 1.** Sintering furnace.

In order to be able to examine metallographically, the samples were sanded with 320, 600, 800, and 1200 mesh sandpapers, respectively. After the sanding process, the samples were polished with the help of diamond paste on the polishing felt. Then, the etching process was carried out in order to see the grain boundaries of the samples more clearly. The composition of the cauterizer used in the etching process consists of 1 ml of HF, 2.5 ml of HNO<sub>3</sub>, and 95 ml of H<sub>2</sub>O. Etching of the samples was done for 10-15 seconds and washed with alcohol and dried. After etching, the microstructure pictures of the samples were examined and illustrated with a Nikon brand optical microscope in the Yahya Eren Advanced Research Laboratory of Bitlis Eren University. In addition, SEM images and EDS analyzes were made with a

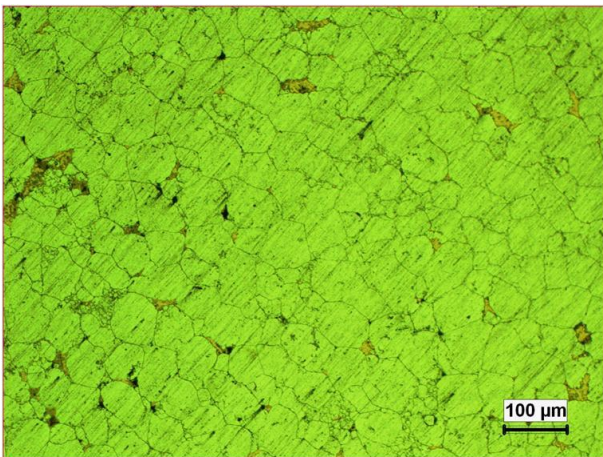
Zeiss scanning electron microscope in Van Yüzüncü Yıl University Science Research and Application Center laboratory. The hardness measurements of the samples were made in the Qness Q10M microhardness device in Vickers (HV0.5) type (Figure 2). XRD analyzes were performed for compound phase detection. XRD analyzes of the samples were made on the Rigaku brand RadB model XRD device in the Scientific and Technological Research Laboratory of İnönü University.



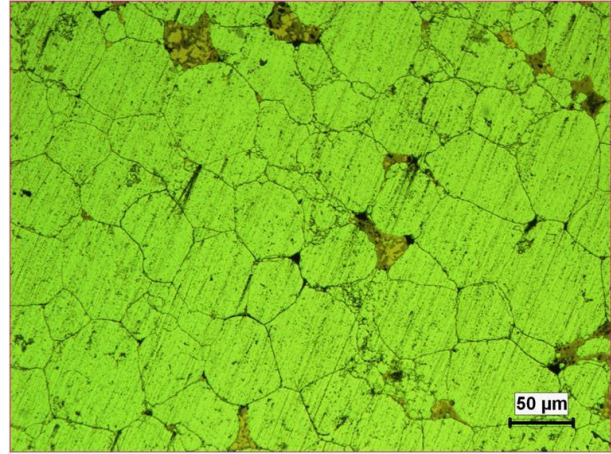
Figure 2. Microhardness tester.

### 3. Results and Discussion

#### 3.1. Microstructure Characterization of Specimens



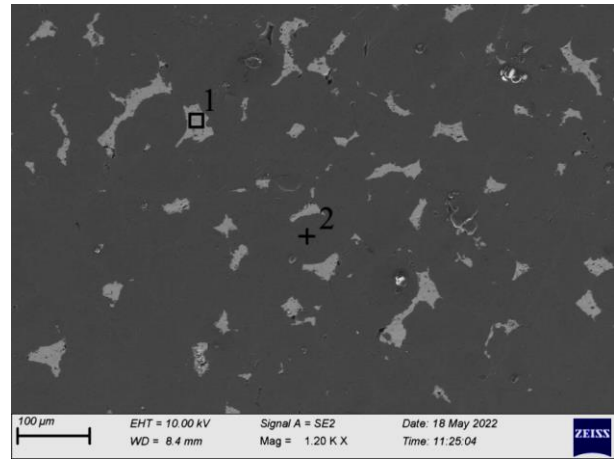
(a)



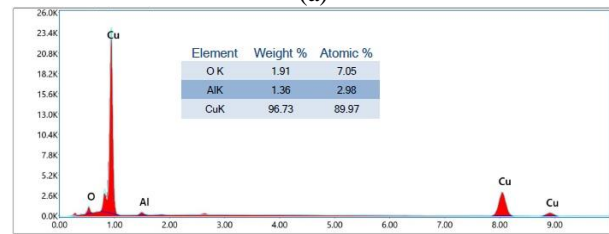
(b)

Figure 3. Optical microstructure pictures taken from Al+5%Cu based sample sintered at 500 °C.

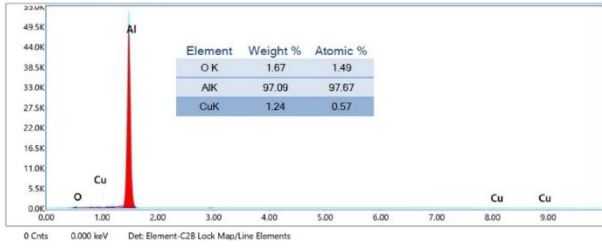
In Figure 3, optical microstructure pictures of the Al+5% Cu sample are shown. Grain boundaries are clearly visible in the microstructure. In the structure consisting of equiaxed grains, it is seen that the element Cu (in red color) is located at the grain boundaries. Porosity is inevitable in samples produced with powder metallurgy. The black-colored pores can be seen in Figure 3.



(a)



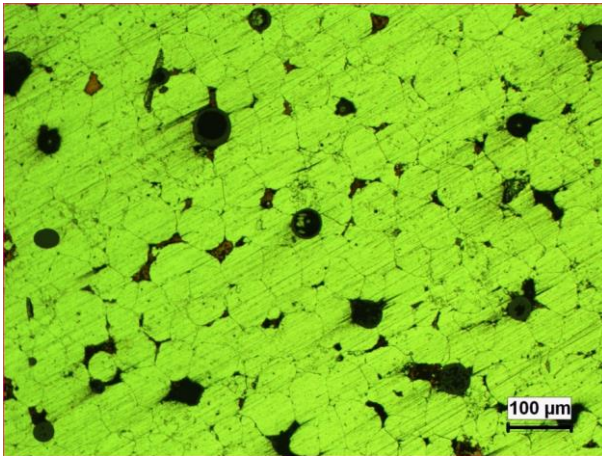
(b)



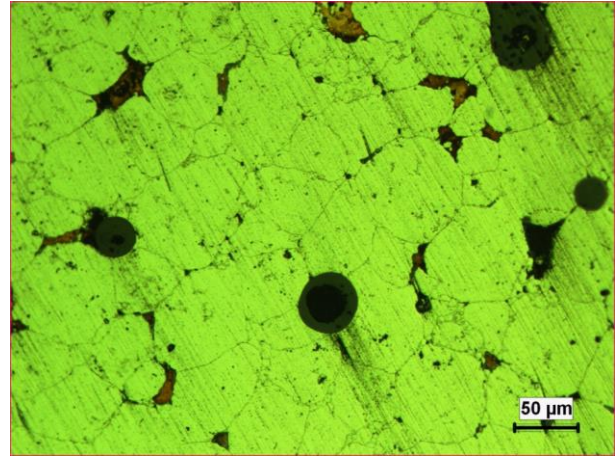
(c)

**Figure 4.** a) SEM photograph taken from Al+5%Cu based sample sintered at 500 °C, b) EDS analysis no. 1 and c) EDS analysis no. 2.

The SEM photograph and EDS analysis results taken from the Al+5%Cu-based sample are shown in Figure 4. It is seen that the structure, which is seen in different colors at the grain boundaries and mentioned in the optical microstructure pictures (Figure 3), consists of a high-weight Cu element by EDS field analysis no 1. In addition, it was determined that 1.36% Al and 1.91% O elements were also present in the analysis. As a result of this EDS, it is thought that  $Cu_xAl_y$  type intermetallic compounds and oxide compounds of Cu and Al elements are formed in area 1. In the EDS analysis at point 2 given in Figure 4-c, the presence of Al matrix structure is seen. In addition, Cu element dissolved in the matrix and a small amount of O element belonging to possible oxide compounds are present at point 2.



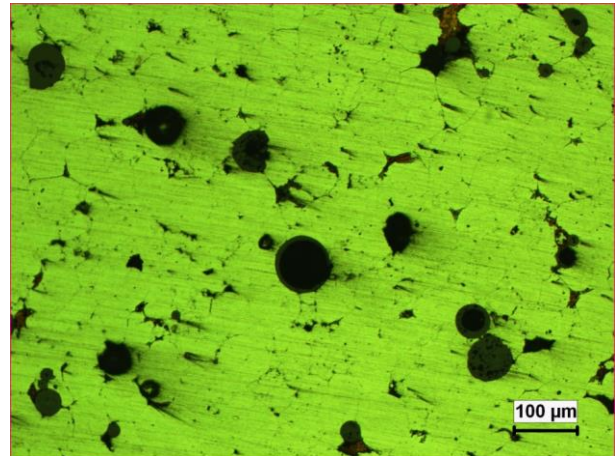
(a)



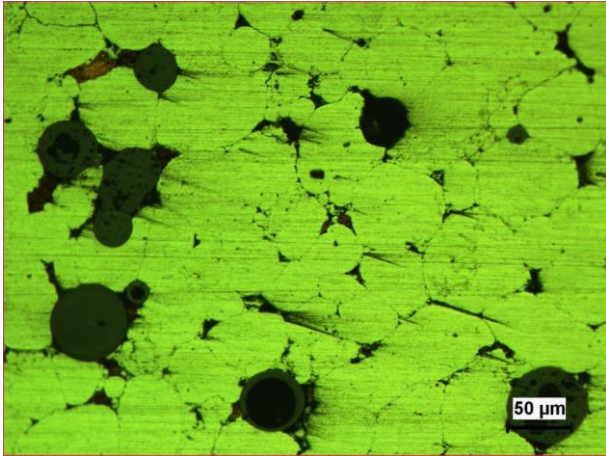
(b)

**Figure 5.** Optical microstructure pictures taken from Al+5%Cu+5%  $ZrO_2$ - $Y_2O_3$  based sample sintered at 500 °C.

Optical microstructure pictures of Al+5%Cu + 5%  $ZrO_2$ - $Y_2O_3$  sample are shown in Figure 5. Grain boundaries can be seen in the microstructure of this sample. In the structure of equiaxed grains, the element Cu (in red color) is located at the grain boundaries. The black colored pores can be seen in Figure 5. The porosity increased more compared to the Al+5%Cu sample with 5% added  $ZrO_2$ - $Y_2O_3$  oxide compound.



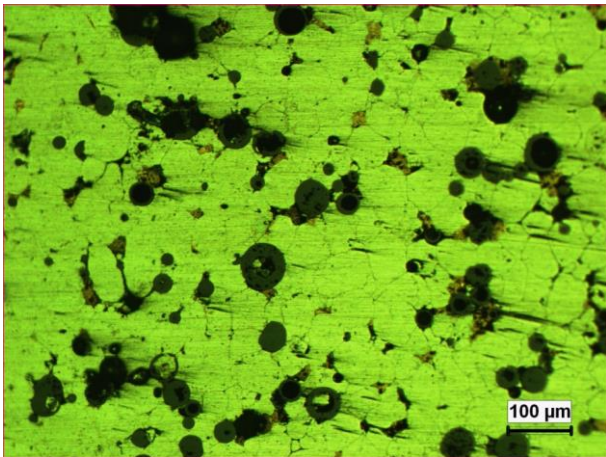
(a)



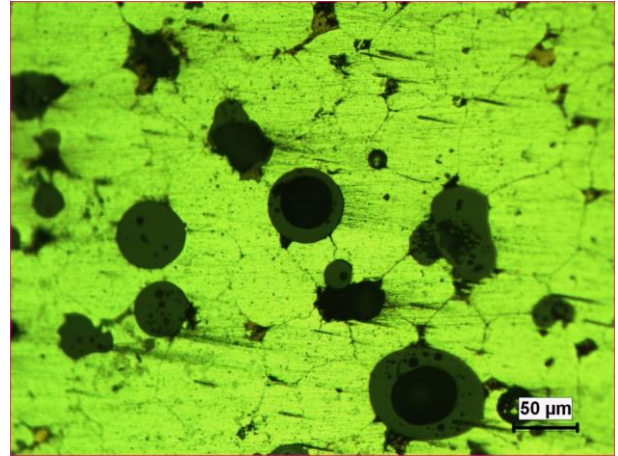
(b)

**Figure 6.** Optical microstructure pictures taken from Al+5% Cu+10% ZrO<sub>2</sub>-Y<sub>2</sub>O<sub>3</sub> based sample sintered at 500 °C.

Figure 6 shows the optical microstructure pictures of the Al + 5% Cu + 10% ZrO<sub>2</sub>-Y<sub>2</sub>O<sub>3</sub> sample. Grain boundaries can be seen in the microstructure of this sample. In the structure consisting of equiaxed grains, the element Cu (in red color) is located at the grain boundaries. It is seen in Figure 6-b that the ZrO<sub>2</sub>-Y<sub>2</sub>O<sub>3</sub> oxide also settles at the grain boundaries during sintering and is found in black colored pores. It can be seen in Figure 6 that the porosity increased even more compared with the samples with Al+5% Cu and Al+5% Cu +5% ZrO<sub>2</sub>-Y<sub>2</sub>O<sub>3</sub>.



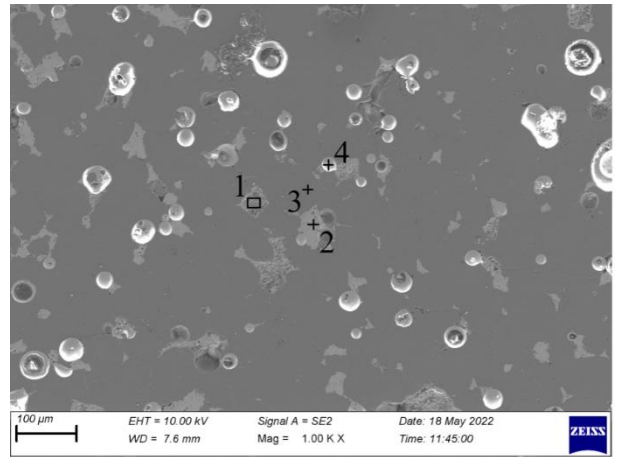
(a)



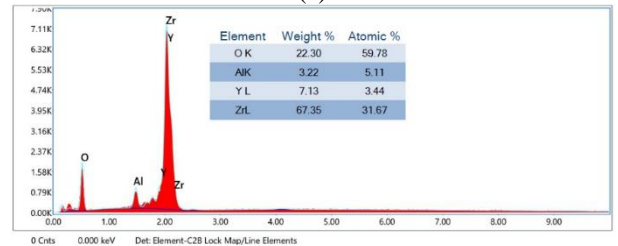
(b)

**Figure 7.** Optical microstructure pictures taken from Al+5% Cu+15% ZrO<sub>2</sub>-Y<sub>2</sub>O<sub>3</sub> based sample sintered at 500 °C.

Optical microstructure pictures of the Al + 5% Cu + 15% ZrO<sub>2</sub>-Y<sub>2</sub>O<sub>3</sub> sample are shown in Figure 7. It is seen in Figure 7-b that the ZrO<sub>2</sub>-Y<sub>2</sub>O<sub>3</sub> oxide also locates at the grain boundaries during sintering. It is seen in Figure 7 that the porosity increased with the addition of 15% ZrO<sub>2</sub>-Y<sub>2</sub>O<sub>3</sub> oxide compound compared to the other samples. It was also observed that pieces of ZrO<sub>2</sub>-Y<sub>2</sub>O<sub>3</sub> dust particles were broken off and voids were formed in the dust particles during sanding.



(a)



(b)

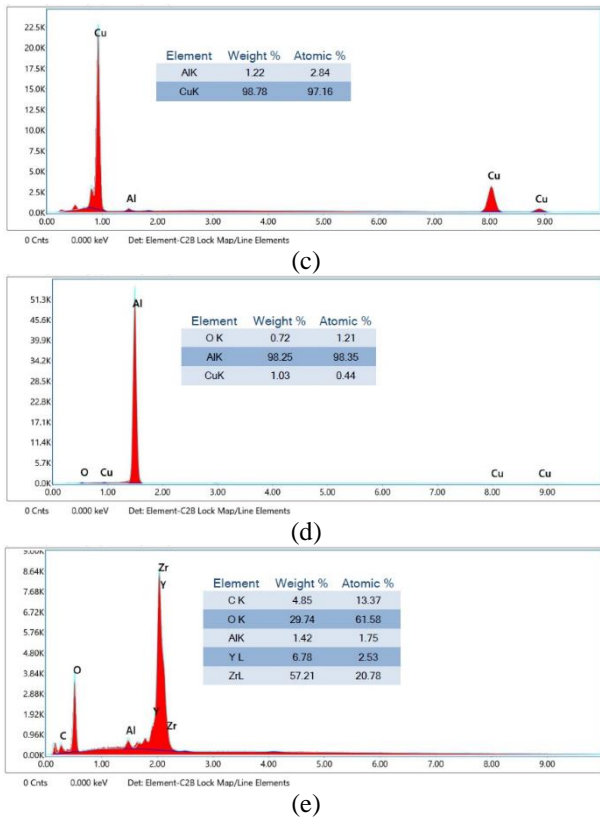


**Figure 8.** Al+5%Cu+15% ZrO<sub>2</sub>-Y<sub>2</sub>O<sub>3</sub> based sample sintered at 500 °C taken from a) SEM photograph, b) EDS analysis no. 1 and c) EDS analysis no. 2 d) EDS analysis no. 3 e) EDS analysis no. 4.

SEM photograph and EDS analysis results taken from Al + 5% Cu + 15% ZrO<sub>2</sub>-Y<sub>2</sub>O<sub>3</sub> sample sintered at 500 °C are shown in Figure 8. EDS analyzes were taken from matrix structure, grain boundaries, and dust particles. The presence of Zr, Y, Al, and O elements is seen in the EDS analysis given in Figure 8-b, taken from the light gray area no 1 in Figure 8-a. It is thought that area no. 1 consists of the added ZrO<sub>2</sub>-Y<sub>2</sub>O<sub>3</sub> powder and the oxide compound of the Al element. The same situation is seen in the EDS analysis taken from point 4 (Figure 8-e). At this point, the presence of Zr, Y, Al, and O elements indicates that ZrO<sub>2</sub>-Y<sub>2</sub>O<sub>3</sub> and Al<sub>2</sub>O<sub>3</sub> type compounds can be formed. In the EDS analysis given in Figure 8-c, Cu can be seen at the point 2. The presence of 98.78% Cu and 1.22% Al elements indicates that Cu<sub>x</sub>Al<sub>y</sub> type intermetallic compounds can be formed. In the EDS analysis given in Figure 8-d, the point 3 is composed of the matrix dust Al element, a small amount of Cu and O elements. At point 3, it is thought that Cu, Al and O elements possible brought about Cu<sub>x</sub>Al<sub>y</sub>, Al<sub>x</sub>O<sub>y</sub> and Cu<sub>x</sub>O<sub>y</sub> type compounds.

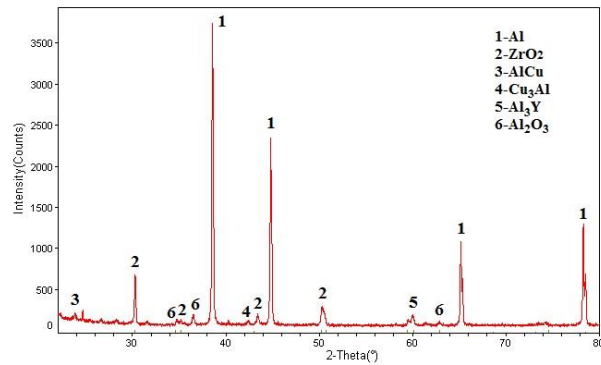


**Figure 9.** XRD analysis of Al+5%Cu+15% ZrO<sub>2</sub>-Y<sub>2</sub>O<sub>3</sub> based sample sintered at 500 °C.

The XRD analysis of the sample obtained from Al+5%Cu+15% ZrO<sub>2</sub>-Y<sub>2</sub>O<sub>3</sub> powder mixture is shown in Figure 9. As a result of XRD analysis, it was determined that different types of compounds were formed. The main phase was determined as the Al element, which is the matrix powder. In addition, AlCu, Cu<sub>3</sub>Al, Al<sub>3</sub>Y, and Al<sub>2</sub>O<sub>3</sub> compounds were formed together with the ZrO<sub>2</sub> compound.

It was observed that the possible compounds related to the detected elements in the EDS analyses (Figure 8) taken from the Al + 5% Cu + 15% ZrO<sub>2</sub>-Y<sub>2</sub>O<sub>3</sub> sample sintered at 500 °C are compatible with the XRD analysis taken from the same sample.

### 3.2. Microhardness Test Results

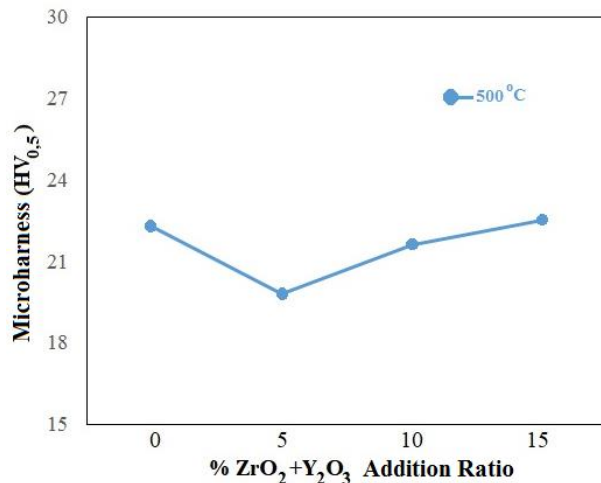


**Figure 10.** Microhardness value of specimens.

The microhardness values of the samples are given in Figure 10. The microhardness value was measured as 22.3 HV from the sample obtained by adding 5% Cu powder to Al. Microhardness values of 18.4 HV in the sample obtained by adding 5% ZrO<sub>2</sub>-Y<sub>2</sub>O<sub>3</sub> powder into Al+5% Cu powder, 21.5 HV in the sample obtained by adding 10% ZrO<sub>2</sub>-Y<sub>2</sub>O<sub>3</sub> powder

into Al+5% Cu powder, and 22.5 HV in the sample obtained by adding 15% ZrO<sub>2</sub>-Y<sub>2</sub>O<sub>3</sub> powder into Al+5% Cu powder were measured. With the addition of ZrO<sub>2</sub>-Y<sub>2</sub>O<sub>3</sub> powder, the number of pores in the microstructure increased in comparison to the sample without ZrO<sub>2</sub>-Y<sub>2</sub>O<sub>3</sub> powder, as can be seen in the microstructure photographs in Figures 3, 5, 6, 7. While the microhardness value was expected to increase with the addition of the ZrO<sub>2</sub>-Y<sub>2</sub>O<sub>3</sub> oxide compound, the microhardness value decreased generally due to the increase in the pore amount. However, a small increase in the microhardness value was observed as the amount of added ZrO<sub>2</sub>-Y<sub>2</sub>O<sub>3</sub> powder increased to 15% (see Fig. 10).

#### **4. Conclusion and Suggestions**

1. With the addition of ZrO<sub>2</sub>-Y<sub>2</sub>O<sub>3</sub> powder, the pores became more prominent at the grain boundaries.
2. In the samples sintered at 500 °C, the microhardness value decreased depending on the number of pores increased with the addition of ZrO<sub>2</sub>-Y<sub>2</sub>O<sub>3</sub> powder.
3. Among the samples, the highest microhardness value was found as a value of 22.5 HV in the sample having 15% ZrO<sub>2</sub>-Y<sub>2</sub>O<sub>3</sub> in Al+5%Cu. The hardness value increased with the increase of the ZrO<sub>2</sub>-Y<sub>2</sub>O<sub>3</sub> ratio.

#### **Acknowledgment**

We would like to thank the Bitlis Eren University Scientific Research Project Coordinator for their support for the Postgraduate Thesis project with the project numbered BEBAP 2022.01.

#### **Contributions of the authors**

This study is a part of Tural HAMİDLİ's master thesis.

#### **Conflict of Interest Statement**

There is no conflict of interest between the authors.

#### **Statement of Research and Publication Ethics**

The study is complied with research and publication ethics.

## References

- [1] H. Su, X. Yan, X. Liu, Y. Ai, K. Ma, R. Li, Z. Zhang, Y. Sun, and S. Liu, "Research on high-temperature mechanical properties and microstructure of powder metallurgical rhenium," *Int. J. of Refractory Metals and Hard Mat.*, Vol. 106, 2022, Art. no. 105861.
- [2] B. Deepanraj, N. Senthilkumar, T. Tamizharasan, "Sintering parameters consequence on microstructure and hardness of copper alloy prepared by powder metallurgy," *Mat. Today: Proc.*, 2021, <https://doi.org/10.1016/j.matpr.2021.06.389>.
- [3] K. Köprülü, N. Mutlu, A. Kurt, B. Gülenç, and Y. Özçatalbaş, "Al+%4,5 Cu Ön karışimli tozların alaşımlanmasına ısıl işlemlerin etkisi," *Gazi University J. of Sci. Part C: Des. and Tech.*, Vol 6, no. 2, 283-293. DOI: 10.29109/http-gujsc-gazi-edu-tr.341722
- [4] N. Kumar, A. Bharti, K. K. Saxena, "A re-investigation: Effect of powder metallurgy parameters on the physical and mechanical properties of aluminium matrix composites," *Mater. Today: Proc.*, Vol. 44, Part 1, 2021, Pages 2188-2193, <https://doi.org/10.1016/j.matpr.2020.12.351>.
- [5] Y. Sayan, V. Venkatesan, E. Guk, H. Wu, and J. S. Kim, "Single-step fabrication of an anode supported planar single-chamber solid oxide fuel cell," *Int. J. Appl. Ceram. Technol.*, vol. 15, no. 6, pp. 1375–1387, 2018, doi: 10.1111/ijac.13012.
- [6] Y. Sayan, J. Kim, and H. Wu, "Residual stress measurement of a single-step sintered planar anode supported SC-SOFC using fluorescence spectroscopy," *Bitlis Eren Üniversitesi Fen Bilim. Derg.*, vol. 11, no. 3, pp. 902–910, 2022, doi: 10.17798/bitlisfen.1139679.
- [7] I. Bahaj, M. Kaddami, A. Dahrouch, N. Labjar, M. Essahli, "The effect of particle content and sintering time on the properties of Al-Al<sub>9</sub>Co<sub>2</sub>-Al<sub>13</sub>Co<sub>4</sub> composites, made by powder metallurgy," *Mater. Today: Proc.*, 2022, <https://doi.org/10.1016/j.matpr.2022.07.220>.
- [8] M. Pul, "Alüminyum 7075 matrisli kompozitlerde SiC, B<sub>4</sub>C Ve TiB<sub>2</sub> takviye elemanlarının mekanik özelliklere etkilerinin karşılaştırılması," *Düzce Üniversitesi Bilim ve Teknoloji Dergisi*, 7 (1), pp. 180-193, 2019. DOI: 10.29130/dubited.431573.
- [9] S. Deniz, "Al<sub>2</sub>O<sub>3</sub> takviyeli alüminyum matrisli kompozit üretimi, mekanik ve fiziksel özellikleri ile mikroyapı Karakterizasyonu," Yıldız Teknik Üniversitesi, Fen Bilimleri Enstitüsü, Doktora Tezi, 2000, İstanbul. 105 sayfa.
- [10] İ. B. Nilüfer, H. Gökçe, H. Çimenoglu, L. Öveçoğlu, "Seryum dioksit ilavesinin zirkonyum dioksit özelliklerine etkisinin incelenmesi," *Mühendis ve Makina*, cilt 55, sayı 652, s. 30-33, 2014.
- [11] H. Karabulut, "Toz metalurjisi yöntemiyle Al<sub>2</sub>O<sub>3</sub>, SiC Ve B<sub>4</sub>C takviyeli al matrisli kompozit üretiminde mekanik alaşımlama süresinin kompozit özelliklerine etkisi," Gazi Üniversitesi Fen Bilimleri Enstitüsü, Doktora Tezi, 2011, Ankara. 119 sayfa.
- [12] M. Aslan, E. Ergul, A. Kaya, H. İ. Kurt, N. F. Yılmaz, "Toz metalurjisi yöntemiyle üretilen Al-MgO kompozitlerin özelliklerine sinterleme sıcaklığının etkisi," *El-Cezeri Fen ve Mühendislik Dergisi* Cilt: 7, No: 3, pp.1131-1139, 2020.
- [13] M. C. Şenel, "Toz metalurjisi yöntemiyle üretilen Saf Al ve Al-B<sub>4</sub>C, Al-Al<sub>2</sub>O<sub>3</sub> kompozitlerin mekanik ve mikroyapı özelliklerinin karşılaştırılması," *Gümüşhane Üniversitesi Fen Bilimleri Enstitüsü Dergisi*, 10 (3), pp.783-795, 2020.
- [14] B. Aktaş, S. Tekeli, G. Küpeli, Y. Bozkurt, Ö. Gülsoy, S. Salman, "Nio / Ysz (Yitriya İle Kararlı Hale Getirilmiş Zirkonya) Seramiklerin Kırılma Tokluğuna Mikro Yapının Etkisi," *Afyon Kocatepe Üniversitesi Fen Bilimleri Dergisi*, Özel Sayı, pp.61-67, 2009.
- [15] I. Gulyaev, V. Kuzmin, E. Kornienko, A. Vyalova, P. Tyryshkin, D. Sergachev, S. Vashchenko, "Plasma spraying of thermal barrier coatings using YSZ powders," *Mater. Today: Proc.*, Vol. 19, Part 5, pp. 2134-2138, 2019. <https://doi.org/10.1016/j.matpr.2019.07.226>.